A line integral-based and mathematically-precise method to partition climate and catchment effects on runoff

Mingguo Zheng[1, 2*]

[1]Guangdong Key Laboratory of Integrated Agro-environmental Pollution Control and Management, Guangdong Institute of Eco-environment Science & Technology, Guangzhou 510650, China
[2]National-Regional Joint Engineering Research Center for Soil Pollution Control and Remediation in South China, Guangzhou 510650, China；
[3]Guangdong Engineering Center of Non-point Source Pollution Prevention Technology, Guangzhou 510650, China;

Correspondence: Mingguo Zheng (mgzheng@soil.gd.cn)

Abstract

It is a common task to partition synergistic impacts of a number of drivers in environmental sciences. However, there is no mathematically precise solution to the partition. Here I presented a line integral-based method, which concerns about the sensitivity to the drivers throughout their evolutionary path so as to ensure a precise partition. The method reveals that the partition depends on both the change magnitude and pathway (timing of change), and not on the magnitude alone unless for a linear system. To illustrate the method, I used the Budyko framework to partition the effects of climatic and catchment conditions on the temporal change in runoff for 21 catchments from Australia and China. The method reduced to the decomposition method when assumed a path along which climate change occurs first followed by an abrupt change in catchment properties. The method re-defines the widely-used concept of sensitivity at a point as the path-averaged sensitivity. The total differential and the complementary methods simply concern about the sensitivity at the initial or/and the terminal state, so that they cannot give precise results. The path-average sensitivity of water yield to climate conditions was found to be stable over time. Space-wise, moreover, it can be readily predicted even in the absence of streamflow observations, whereby facilitates evaluation of future climate effects on streamflow. As a mathematically accurate solution, the method provides a generic tool to conduct the quantitative attribution analyses.

Keywords: Runoff; Climate change; Human activities; Attribution analysis; Budyko

1 Introduction

It is often needed to quantify the relative roles of a few drivers to the observed changes of interest in environmental sciences. In the hydrology community, diagnosing the relative contributions of climate change and human activities to runoff is of great relevance to the researchers and managers as both climate and human activities have pose global-scale impact on hydrologic cycle and water resources (Barnett *et al.*, 2008; Xu *et al.*, 2014; Wang and Hejazi, 2001). Unfortunately, the quantitative attribution analysis of the runoff changes remains a challenge (Wang and Hejazi, 2001; Berghuijs and Woods, 2016; Zhang *et al.*, 2016); this is to a considerable degree due to a lack of a mathematically precise method to decouple synergistic and often confounding impacts of climate change and human activities.

Numerous studies have detected the long term variability in runoff and attempted to partition the effects of climate change and human activities by means of various methods (Dey and Mishra, 2017). Among them are the paired-catchments method and the hydrological modeling method. The paired-catchment method is believed to be able to filter the effect of climatic variability and thus isolate the runoff change induced by vegetation changes (Brown *et al.*, 2005). However, the method is capital intensive. Particularly, it generally involves small catchments and is challenged when extrapolating to large catchments (Zhang *et al.*, 2011). The physical-based hydrological models often suffer from limitations including high data requirement, labor-intensive calibration and validation processes, and inherent uncertainty and interdependence in parameter estimations (Binley *et al.*, 1991; Wang *et al.*, 2013; Liang *et al.*, 2015). Interest then turns to the conceptual models over recent years, such as the Budyko-type equations (see Section 2.1).

Within the Budyko framework, a large number of studies (Roderick and Farquhar, 2011; Zhang *et al.*, 2016) have used the total differential of runoff (i.e. dR, where R represents runoff) as a proxy for the runoff change (i.e. ΔR) and further evaluated hydrological responses to climate change and human activities (hereafter called the total differential method). However, dR is essentially a first-order approximation of ΔR (Fig. 1(a)). It has been shown that the approximation has caused an error of the climate impact on runoff ranging from 0 to 20 mm (or -118 to 174%) over China (Yang *et al.*, 2014). The total differential method directly used the partial derivatives of runoff as the sensitivities of runoff to climate and catchment conditions. Most studies applied the forward approximation of the runoff change, *i.e.*, using the sensitivities at the initial state while calculation (e.g. Roderick and Farquhar, 2011). The elasticity method proposed by Schaake (1990) is also based on the total differential expression (Sankarasubramanian *et al.*, 2001; Zheng *et al.*, 2009). The method uses the “elasticity” concept to assess the climate sensitivity of runoff. The elasticity coefficients, however, have been estimated in an empirical way and is not physically sound (Roderick and Farquhar, 2011; Liang *et al.*, 2015).

The so-called decomposition method developed by Wang and Hejazi (2011) has also been widely used. The method assumes that climate changes drive a shift along a Budyko curve and then human interferences cause a vertical shift from the Budyko curve to another (Fig. 1(b)). Under this assumption, the method extrapolates the Budyko models calibrated using observations of the reference period, in which human impacts remain minimal, to determine the human-induced changes in runoff occurred during the evaluation period.

Recently, Zhou *et al.* (2016) established a Budyko complementary relationship for runoff and applied it to partitioning the climate and catchment effects. Superior to the total differential method, the method culminates with yielding a no-residual partition. Nevertheless, the method depends on a given weighted factor, which is determined in an empirical but not a precise way. Furthermore, Zhou *et al.* (2016) argued that the partition is not unique in the Budyko framework as the path of the climate and catchment changes cannot be uniquely identified.

A precise partition remains difficult even given a precise mathematical model. This can be illustrated by using a precise hydrology model R = f(x, y), where x and y climate factors and catchment characteristics respectively. We assumed that R changes by ΔR when x changes by Δx and y by Δy , *i.e.* $\Delta R = f(x+\Delta x, y+\Delta y) - f(x, \mathrm{y})$. To determine the effect of x on ΔR , *i.e.* ΔR_x , a common practice is to assume that y remains constant when x changes by Δx . We thus get: $\Delta R_x = f(x+\Delta x, y) - f(x, y)$. Similarly, we can get: $\Delta R_y = f(x, y+\Delta y) - f(x, y)$. Although the derivation seems quite reasonable, it is problematic as the sum of ΔR_x and ΔR_y is not equal to ΔR . Further examination shows that a variable's effect on R seems to differ depending on the changing path. For example, $\Delta R_x = f(x+\Delta x, y) - f(x, y)$ and $\Delta R_y = f(x+\Delta x, y+\Delta y) - f(x+\Delta x, y)$ if x changes first and y subsequently (Note that the partition is precise with the sum of ΔR_x and ΔR_y equaling ΔR now). If y changes first and x subsequently, the partition then becomes: $\Delta R_x = f(x+\Delta x, y+\Delta y) - f(x, y+\Delta y)$ and $\Delta R_y = f(x, y+\Delta y) - f(x, y)$. In case of x and y changing simultaneously, unfortunately, current literature seems not to provide a mathematically precise solution.

The aims of this work are to propose a mathematically precise method to conduct quantitative attribution to drivers. The method is based on the line integer (called the LI method hereafter) and takes account of the sensitivity throughout the evolutionary path of the drivers rather than at a point as the total differential method does. In this way, the method revises the widely-used concept of sensitivity at a point as the path-averaged sensitivity. To present and evaluate the method, I decomposed the relative influences of climate and catchment conditions on runoff within the Budyko framework using data from 21 catchments from Australia and China. I also examined the spatio-temporal variability of the path-averaged sensitivities of runoff to climatic and catchment conditions and assessed their spatio-temporal predictability.

2 Methodology

2.1 The Budyko Framework and the MCY equation

Budyko (1974) argued that the mean annual evapotranspiration (E) is largely determined by water and energy balance of a catchment. Using precipitation (P) and potential evapotranspiration (E_0) as proxies for water and energy availabilities respectively, the Budyko framework relates evapotranspiration losses to the aridity index defined as the ratio of E_0 over P. The Budyko framework has gained wide acceptance in the hydrology community (Berghuijs and Woods, 2016; Sposito, 2017). Over past decades, a number of equations have been developed to describe the framework. Among them, the Mezentsev-Choudhury-Yang's equation (Mezentsev, 1955; Choudhury, 1999; Yang *et al.*, 2008) (Called the MCY equation hereafter) has been widely accepted and was used here:

$$\frac{E}{P} = \frac{E_0/P}{(1+(E_0/P)^n)^{1/n}} \tag{1}$$

where $n \in (0, \infty)$ is an integration constant that is dimensionless, and represents catchment properties. Eq. (3) requires a relative long time scale whereby the water storage of a catchment is negligible and the water balance equation reduces to be $R = P - E$. Here I adopted a "tuned" n value that can get exact agreement between the calculated E by Eq. (1) and that actually encountered ($= P - R$).

The partial differentials of R with respect to P, E_0, and n are given as:

$$\frac{\partial R}{\partial P} = R_P(P, E_0, n) = 1 - \frac{E_0^{n+1}}{(P^n + E_0^n)^{1/n}} \tag{2a}$$

$$\frac{\partial R}{\partial E_0} = R_{E_0}(P, E_0, n) = -\frac{P^{n+1}}{(P^n + E_0^n)^{1/n}} \tag{2b}$$

$$\frac{\partial R}{\partial n} = R_n(P, E_0, n) = \frac{-E_0 P n^{-1}}{(P^n + E_0^n)^{1/n}} \left[\frac{\ln(P^n + E_0^n)}{n} - \frac{P^n \ln P + E_0^n \ln E_0}{P^n + E_0^n} \right] \tag{2c}$$

2.2 The theory of the line integral-based method

To present the LI method, we start by considering an example of a two-variable function $z = f(x, y)$, which has continuous partial derivatives $\partial z / \partial x = f_x(x, y)$ and $\partial z / \partial y = f_y(x, y)$. Suppose that x and y varies along a smooth curve L (e.g. $\overset{\frown}{AC}$ in Fig. 1(c)) from the initial state (x_0, y_0) to the terminal state (x_N, y_N), and z co-varies from z_0 to z_N. Let $\Delta z = z_N - z_0$, $\Delta x = x_N - x_0$, and $\Delta y = y_N - y_0$. Our goal is to seek for a mathematical solution to quantify the effects of Δx and Δy on Δz, i.e. Δz_x and Δz_y. Δz_x and Δz_y should be subject to the constraint $\Delta z_x + \Delta z_y = \Delta z$.

As shown in Fig. 1(c), points $M_1(x_1, y_1)$,…, $M_{N-1}(x_{N-1}, y_{N-1})$ partition L into N distinct segments. Let $\Delta x_i = x_{i+1} - x_i$, $\Delta y_i = y_{i+1} - y_i$, and $\Delta z_i = z_{i+1} - z_i$. For each segment, Δz_i can be approximated as the total differential dz_i: $\Delta z_i \approx dz_i = f_x(x_i, y_i)\Delta x_i + f_y(x_i, y_i)\Delta y_i$. We then have: $\Delta z = \sum_{i=1}^{N} \Delta z_i \approx \sum_{i=1}^{N} f_x(x_i, y_i)\Delta x_i + \sum_{i=1}^{N} f_y(x_i, y_i)\Delta y_i$. We thus obtain an approximation of Δz_x and Δz_y: $\Delta z_x \approx \sum_{i=1}^{N} f_x(x_i, y_i)\Delta x_i$ and $\Delta z_y \approx \sum_{i=1}^{N} f_y(x_i, y_i)\Delta y_i$. Define τ as the maximum length among the N segments. The smaller the value of τ, the closer to Δz_i the value of dz_i, and then the better the approximations are. The approximations becomes exact in the limit $\tau \to 0$. Taking the limit $\tau \to 0$ then turns sum into integrals and gives a precise expression (it is an informal derivation and please see Appendix A for a formal one): $\Delta z = \lim_{\tau \to 0} \sum_{i=1}^{N} f_x(x_i, y_i)\Delta x_i + \lim_{\tau \to 0} \sum_{i=1}^{N} f_y(x_i, y_i)\Delta y_i = \int_L f_x(x, y)dx + \int_L f_y(x, y)dy$, where $\int_L f_x(x, y)dx = \lim_{\tau \to 0} \sum_{i=1}^{N} f_x(x_i, y_i)\Delta x_i$ and $\int_L f_y(x, y)dy = \lim_{\tau \to 0} \sum_{i=1}^{N} f_y(x_i, y_i)\Delta y_i$ denote the line integral of f_x and f_y along L (termed integral path) with respect to x and y, respectively. $\int_L f_x(x, y)dx$ and $\int_L f_y(x, y)dy$ exist provided that f_x and f_y are continuous along L. We thus obtain a precise evaluation of Δz_x and Δz_y:

$$\Delta z_x = \int_L f_x(x, y)dx \tag{3a}$$

$$\Delta z_y = \int_L f_y(x, y)dy \, . \qquad (3b)$$

Unlike the total differential method, the sum of Δz_x and Δz_y persistently equals Δz (Appendix B). If $f(x, y)$ is linear, then f_x and f_y are constant. Define $C_x = f_x(x, y)$ and $C_y = f_y(x, y)$, we have $\Delta z_x = C_x \Delta x$ and $\Delta z_y = C_y \Delta y$. Δz_x and Δz_y are thus independent of L. If $f(x, y)$ is non-linear, however, both Δz_x and Δz_y varies with L, as was exemplified in Appendix C. Hence, the initial and the terminal states, together with the path connecting them, determine the resultant partition unless $f(x, y)$ is linear.

The mathematical derivation above applies to a three-variable function as well. By doing the line integrals for the MCY equation, we obtain the desired results:

$$\Delta R_P = \int_L \frac{\partial R}{\partial P} dP \qquad (4a)$$

$$\Delta R_{E_0} = \int_L \frac{\partial R}{\partial E_0} dE_0 \qquad (4b)$$

$$\Delta R_n = \int_L \frac{\partial R}{\partial n} dn \qquad (4c)$$

where ΔR_P, ΔR_{E_0}, and ΔR_n denotes the effects on runoff change of P, E_0, and n, respectively. The sum of ΔR_P and ΔR_{E_0} represents the effect of climate change, and ΔR_n are often related to human activities although it probably includes the effects of other factors, such as climate seasonality (Roderick and Farquhar, 2011; Berghuijs and Woods, 2016). L denotes a three-dimensional curve along which climate and catchment changes have occurred. I approximated L as a union of a series of line segments. ΔR_P, ΔR_{E_0}, and ΔR_n were finally figured out by summing up the integrals along each of the line segments (see Section 2.3).

2.3 Using the LI method to determine ΔR_P, ΔR_{E_0}, and ΔR_n within the Budyko Framework

1) Determining ΔR_P, ΔR_{E_0}, and ΔR_n assuming a linear integral path

.Given two consecutive periods and assumed that the catchment state has evolved from (P_1, E_{01}, n_1) to (P_2, E_{02}, n_2) along a straight line L. Let $\Delta P = P_2 - P_1$, $\Delta E_0 = E_{02} - E_{01}$, and $\Delta n = n_2 - n_1$, then the line L is given by parametric equations: $P = \Delta P t + P_1$, $E_0 = \Delta E_0 t + E_{01}$, $n = \Delta n t + n_1$, $t \in [0,1]$. Given the equations, Eq. (2) becomes a one-variable function of t, i.e., $\partial R / \partial P = R_p(t)$, $\partial R / \partial E_0 = R_{E_0}(t)$, and $\partial R / \partial n = R_n(t)$. Then, ΔR_P, ΔR_{E_0}, and ΔR_n can be evaluated as:

$$\Delta R_P = \int_L \frac{\partial R}{\partial P} dP = \int_0^1 R_P(t) d(\Delta P t + P_1) = \Delta P \int_0^1 R_P(t) dt \qquad (5a)$$

$$\Delta R_{E_0} = \int_L \frac{\partial R}{\partial E_0} dE_0 = \int_0^1 R_{E_0}(t) d(\Delta E_0 t + E_{01}) = \Delta E_0 \int_0^1 R_{E_0}(t) dt \qquad (5b)$$

$$\Delta R_n = \int_L \frac{\partial R}{\partial n} dn = \int_0^1 R_n(t) d(\Delta n t + n_1) = \Delta n \int_0^1 R_n(t) dt \qquad (5c)$$

Unfortunately, I cannot figure out the antiderivatives of $R_P(t)$, $R_{E_0}(t)$, and $R_n(t)$ and have to make approximate calculations. As the discrete equivalent of integration is summation, we can approximate integration as summation. I divided the $t \in [0,1]$ interval into 1000 subintervals of the same width, thereby setting dt identically equal to 0.001, and then then calculated $R_P(t)dt$, $R_{E_0}(t)dt$, and $R_n(t)dt$ for each subinterval. Let $t_i = 0.001i, i \in [0, 999]$ and is integer-valued, ΔR_P, ΔR_{E_0}, and ΔR_n was approximated as:

$$\Delta R_P \approx 0.001 \Delta P \sum_{i=0}^{999} R_P(t_i) \quad (6a)$$

$$\Delta R_{E_0} \approx 0.001 \Delta E_0 \sum_{i=0}^{999} R_{E_0}(t_i) \quad (6b)$$

$$\Delta R_n \approx 0.001 \Delta n \sum_{i=0}^{999} R_n(t_i) \quad (6c)$$

2) Dividing the evaluation period into a number of subperiods

I first determine a change point and divide the whole observation period into the reference and evaluation periods. To determine the integral path, the evaluation period is further divided into a number of subperiods. The Budyko framework assumes a steady state condition of a catchment and therefore requires no change in soil water storage. Over a time period of 5-10 years, it is reasonable to assume that changes in soil water storage are sufficiently small (Zhang *et al.*, 2001). Here I divided the evaluation period into a number of 7-year subperiods with the exception for the last one, which varied from 7 to 13 years in length depending on the length of the evaluation period.

3) Determining ΔR_P, ΔR_{E_0}, and ΔR_n by approximating the integral path as a series of line segments

As did in Fig. 1(c), a curve can be approximated as a series of line segments. For a short period, the integral path L can be considered as linear, which implies a temporally invariant change rate. For a long period, in which the change rate usually varies over time, L can be fitted using a number of line segments. Given a reference period and an evaluation period comprising N subperiods, I assumed that the catchment state evolved from (P_0, E_{00}, n_0), …, (P_i, E_{0i}, n_i), …, to (P_N, E_{0N}, n_N), where the subscript "0" denotes the reference period, and "i" and "N" denotes the ith and the last subperiods of the evaluation period, respectively. I used a series of line segments L_1, L_2, …, L_N to approximate the integral path L, where L_1 connects (P_0, E_{00}, n_0) with(P_1, E_{01}, n_1), L_i connects points ($P_{i\text{-}1}$, $E_{0,i\text{-}1}$, $n_{i\text{-}1}$) with (P_i, E_{0i}, n_i), and the initial point of L_{i+1} is the terminal point of L_i and. Then ΔR_P, ΔR_{E_0}, and ΔR_n are evaluated as the sum of the integrals along each of the line segments, which was calculated using Eq. (6).

2.4 The total-differential, decomposition and complementary methods

To evaluate the LI method, I compared it with the decomposition method, the total differential method, and the complementary method. The total differential method approximated ΔR as dR (Fig. 1(a)):

$$\Delta R \approx dR = \frac{\partial R}{\partial P}\Delta P + \frac{\partial R}{\partial E_0}\Delta E_0 + \frac{\partial R}{\partial n}\Delta n = \lambda_P \Delta P + \lambda_{E_0}\Delta E_0 + \lambda_n \Delta n \quad (7)$$

where $\lambda_P = \partial R / \partial P$, $\lambda_{E_0} = \partial R / \partial E_0$, and $\lambda_n = \partial R / \partial n$, representing the sensitivity coefficient of R with respect to P, E_0, and n, respectively. Within the total differential method, $\Delta R_P = \lambda_P \Delta P$, $\Delta R_{E_0} = \lambda_{E_0} \Delta E_0$, and $\Delta R_n = \lambda_n \Delta n$. I used the forward approximation, *i.e.* substituting the observed mean annual values of the reference period into Eq. (2), to estimate λ_P, λ_{E_0}, and λ_n, as did in most studies (Roderick and Farquhar, 2011; Yang and Yang, 2011; Sun *et al.*, 2014).

The decomposition method (Wang and Hejazi, 2011) calculated ΔR_n as follows:

$$\Delta R_n = R_2 - R_2^{'} = (P_2 - E_2) - (P_2 - E_2^{'}) = E_2^{'} - E_2 \quad (8)$$

where R_2, P_2, and E_2 represents the mean annual runoff, precipitation and evapotranspiration of the evaluation period; and $R_2^{'}$ and $E_2^{'}$ represents the mean annual runoff and evapotranspiration respectively, given the climate conditions of the evaluation period and the catchment conditions of the reference period. Both E_2 and $E_2^{'}$ were calculated by Eq. (1), but using n values of the evaluation period and the reference period respectively.

The complementary method (Zhou *et al.*, 2016) uses a linear combination of the complementary relationship for runoff to determine ΔR_P, ΔR_{E0}, and ΔR_n:

$$\begin{aligned}\Delta R = & a\left[\left(\frac{\partial R}{\partial P}\right)_1 \Delta P + \left(\frac{\partial R}{\partial E_0}\right)_1 \Delta E_0 + P_2 \Delta\left(\frac{\partial R}{\partial P}\right) + E_{0,2} \Delta\left(\frac{\partial R}{\partial E_0}\right)\right] \\ & +(1-a)\left[\left(\frac{\partial R}{\partial P}\right)_2 \Delta P + \left(\frac{\partial R}{\partial E_0}\right)_2 \Delta E_0 + P_1 \Delta\left(\frac{\partial R}{\partial P}\right) + E_{0,1} \Delta\left(\frac{\partial R}{\partial E_0}\right)\right]\end{aligned} \quad (9)$$

where the subscript 1 and 2 denotes the reference and the evaluation periods, respectively. a is a weighting factor and varies from 0 to 1. As suggested by Zhou *et al.* (2016), I set a = 0.5. Equation (9) thus gave an estimation of ΔR_P, ΔR_{E0}, and ΔR_n as follows:

$$\Delta R_P = 0.5 \Delta P\left[\left(\frac{\partial R}{\partial P}\right)_1 + \left(\frac{\partial R}{\partial P}\right)_2\right] \quad (10a)$$

$$\Delta R_{E0} = 0.5 \Delta E_0\left[\left(\frac{\partial R}{\partial E_0}\right)_1 + \left(\frac{\partial R}{\partial E_0}\right)_2\right] \quad (10b)$$

$$\Delta R_n = 0.5 \Delta\left(\frac{\partial R}{\partial P}\right)(P_1 + P_2) + 0.5 \Delta\left(\frac{\partial R}{\partial E_0}\right)(E_{0,1} + E_{0,2}) \quad (10c)$$

2.5 Data

I collected data of runoff and climate of 21 selected catchments from previous studies (Table 1). The change-point years gave in the studies was directly used to determine the reference and evaluation periods for the LI method. As mentioned above, the LI method further divides the evaluation period into a number of subperiods. For the sake of comparison, the last subperiod of the evaluation period was used as the evaluation period for the decomposition, the total differential and the complementary methods (It can be equally considered that all methods used the last subperiod as the evaluation period, but the LI method cares about the intermediate period between the reference and the evaluation periods and the others do not). Nine of the 21 catchments had a reference period comprising only one subperiod (Table 1), and the others had two to seven ones.

The 21 selected catchments were located in diverse climates and landscapes. Among them, 14 are from Australia and 7 from China (Table 1). The catchments spanned from tropical to subtropical and temperate and from humid to semi-humid and semi-arid regions, with mean annual rainfall varying from 506 to 1014 mm and potential evaporation from 768 to 1169 mm. The index of dryness ranges between 0.86 and 1.91. The catchment areas vary by five orders of magnitude from 1.95 to 121,972 with a median 606 km^2. The key data includes annual runoff, precipitation, and potential evaporation. The record length varied between 15 and 75 with a median of 35 years. Among the 21 catchments, the changes from the reference to the evaluation period ranged between -271 and 79 mm yr^{-1} for precipitation, and -35 and 41 mm yr^{-1} for potential evaporation (Table 2). The coeval change in the parameter *n* of the MCY equation ranged between -0.2 to 2.53. All of the catchments experienced both climate change and land cover change over the observation period. The mean annual streamflow reduced for all of them, by from 0.43 to 229 with a median 38 mm yr^{-1}. More details of data and the catchments can be found in Zhang *et al.* (2011), Sun *et al.* (2014), Zhang *et al.* (2010), Zheng *et al.* (2009), Jiang *et al.* (2015), and Gao *et al.* (2016).

3 Results

3.1 Comparisons with existing methods

The LI method first partitions the whole observation period into the reference and evaluation periods, then further divides the latter into a number of subperiods and evaluates the contributions to runoff from climate and catchment changes for each subperiod, and finally adds up the derived contributions. Table 3 lists all of the resultant values of ΔR_P, ΔR_{E_0}, and ΔR_n of the LI method, together with the three other methods.

Fig. 2(a) compares the resultant ΔR_n of the LI method and the decomposition method. Although they are quite similar, the discrepancies between them can be up to >20 mm yr^{-1}. The decomposition method assumes that climate change occurs first and then human interferences cause a sudden change in catchment properties (Fig. 1(b)). Such a fictitious path is identical to the broken line AB+BC in Fig. 1(c), provided that *x* represents climate factors and *y* catchment properties. As a result, the decomposition method can be considered as a special case of the LI method when adopting the broken line AB+BC in Fig. 1(c) as the integral path, as was demonstrated clearly in Fig. 2(b).

The total differentiae method is predicated on an approximate equation, *i.e.* Eq. (7). The LI method reveals that the precise form of the equation is $\Delta R = \overline{\lambda_P}\Delta P + \overline{\lambda_{E_0}}\Delta E_0 + \overline{\lambda_n}\Delta n$ (i.e. Eq. (D2) in Appendix D), where $\overline{\lambda_P}$, $\overline{\lambda_{E_0}}$ and $\overline{\lambda_n}$ (Table 4) denote the path-averaged sensitivity of *R* to *P*, E_0, and *n*, respectively. All points along the path have the same weight in determining $\overline{\lambda_P}$, $\overline{\lambda_{E_0}}$ and $\overline{\lambda_n}$. To determine them, the total differential method utilizes only the initial state and the complementary method utilizes the initial and the terminal states. Neglecting the intermediate states between the initial and the terminal ones possibly results in a reverse trend estimation (see ΔR_{E_0} for Catchment NO. 1 in Table 3). Although the elasticity method exploits information contained over the entire observation period (e.g. Zheng *et al.*, 2009; Wang *et al.*, 2013), the resultant descriptive statistics of climate elasticity may not be robust (Roderick and Farquhar, 2011; Liang *et al.*, 2015).

Superior to the total differential method, the sum of ΔR_P, ΔR_{E_0}, and ΔR_n always equaled to ΔR for the LI method. Examination of the subperiods revealed that $\partial R/\partial n$ was more temporally variable than $\partial R/\partial P$ and $\partial R/\partial E_0$ (discussed below). For this reason, ΔR_n showed considerable discrepancies between the two methods but ΔR_P as well as ΔR_{E_0} matched well between the two methods (Fig. 3).

As with the LI method, the complementary method produced ΔR_P, ΔR_{E_0}, and ΔR_n that exactly add up to ΔR. Although its resultant ΔR_P, ΔR_{E_0}, and ΔR_n were all in good agreement with the LI method

(Fig. 4), the LI method often yielded values beyond the bounds given by the complementary method (Fig. 5); this is because the initial and terminal states are not equivalent to the maximum and minimum values over the integral path.

3.2 The spatio-temporal variability of the path-averaged sensitivities

$\overline{\lambda_P}$, $\overline{\lambda_{E_0}}$ and $\overline{\lambda_n}$ implies the average runoff change induced by a unit change in P, E_0 and n, respectively (Appendix D). Their spatio-temporal variability is relevant to the prediction of the runoff change. To evaluate their temporal variabilities, I calculated $\overline{\lambda_P}$, $\overline{\lambda_{E_0}}$ and $\overline{\lambda_n}$ for each subperiod of the evaluation period and assessed their deviation from those for the whole evaluation period. As shown in Fig. 6, the deviation was rather limited for $\overline{\lambda_P}$ (averaged 8.6%) and $\overline{\lambda_{E_0}}$ (averaged 13%), but was considerable for $\overline{\lambda_n}$ (averaged 41%). Hence, it seems quite safe to predict the future climate effects on runoff using earlier $\overline{\lambda_P}$ and $\overline{\lambda_{E_0}}$, but care must be taken when using earlier $\overline{\lambda_n}$ to predict future catchment effect on runoff.

Different from the temporal variability, $\overline{\lambda_P}$, $\overline{\lambda_{E_0}}$ and $\overline{\lambda_n}$ all varied greatly, by up to several or even ten folds, between the studied catchments (Table 4). It was found that there were good correlations between $\overline{\lambda_P}$ and P, between $\overline{\lambda_{E_0}}$ and P, and between $\overline{\lambda_n}$ and n (Fig. 7). Fig. 8 shows that Eq. (2) reproduced $\overline{\lambda_P}$, $\overline{\lambda_{E_0}}$ and $\overline{\lambda_n}$ very well taking the long-term means of P, E_0, and n as inputs, a fact that the dependent variable approached its average if setting the independent variables to be their averages. The finding is of relevance to the spatial prediction of $\overline{\lambda_P}$, $\overline{\lambda_{E_0}}$ and $\overline{\lambda_n}$; moreover, it would greatly facilitate the prediction of future climate effect on runoff as $\overline{\lambda_P}$ and $\overline{\lambda_{E_0}}$ was rather stable over time as previously mentioned.

Runoff data and in turn, the parameter n in the MCY equation, are often unavailable. It is thus desirable to make predictions of $\overline{\lambda_P}$, $\overline{\lambda_{E_0}}$ and $\overline{\lambda_n}$ in the absence of the parameter n. I developed three strategies as follows: 1) using Eq. (2) and assuming n = 2 as n is typically in a small range from 1.5 to 2.6 (Roderick and Farquhar, 2011); 2) using P and E_0 to establish regression models; 3) using the aridity index to establish regressions as it appeared to be more correlated with both $\overline{\lambda_P}$ and $\overline{\lambda_{E_0}}$ than P and E_0 (Fig. 7). As shown in Fig. 9, the three strategies have similar performance although the second one seems to perform better. All of the strategies gave acceptable predictions of $\overline{\lambda_P}$ and $\overline{\lambda_{E_0}}$, but rather poor results for $\overline{\lambda_n}$ as it was primarily controlled by n (Fig. 7). It was thus needed to seek more sophisticated approaches to predict the future catchment effect on runoff in the absence of runoff observations.

4 Discussion

The LI method re-defines the widely-used concept of sensitivity at a point as the path-averaged sensitivity. The method highlights the role of the evolutionary path in determining the resultant partition. Yet, it seems that no studies have taken into account the path issue while evaluating the relative influences of drivers. Compared with the existing methods, the limit of the LI method is high data requirement for obtaining the evolutionary path. When the data are unavailable, the complementary method can be considered as an alternative. First, the complementary method offer results free of residuals; in addition, it employs both data of the reference and the evaluation periods to determine the sensitivities, thereby generally yielding values closer to the path-averaged sensitivities than the total differentiae method.

While using the Budyko models, a reasonable time scale is relevant to meet the assumption that changes in catchment water storage are small relative to the magnitude of fluxes of *P*, *R* and *E* (Donohue et al., 2007; Roderick and Farquhar, 2011). The present study selected seven years as most studies have suggested a time period of 5-10 years (Zhang *et al*., 2001; Zhang *et al*., 2016; Wu *et al*., 2017a; Wu *et al*., 2017b; Li *et al*., 2017) or even one year (Roderick and Farquhar, 2011; Sivapalan *et al*., 2011; Carmona *et al*., 2014; Ning *et al*., 2017). Nevertheless, some studies asserted that the time period should be longer than ten years (Li *et al*., 2016; Dey and Mishra, 2017). If this is the case, the high temporal variation of $\overline{\lambda_n}$ shown in Fig. 6 might be caused by water storage changes, rather than actual changes in the catchment properties. The uncertainty should be addressed. Using the Gravity Recovery and Climate Experiment (GRACE) satellite gravimetry, Zhao *et al*.(2011) detected the water storage variations for three largest river basins of China, namely, Yellow, Yangtze, and Zhujiang. The Yellow River mostly drains an arid and semiarid region (*P*, 450mm; *R*, 70 mm; *E*, 380mm), and the Yangtze (*P*, 110mm; *R*, 550 mm; *E*, 550mm) and the Zhujiang river basins (*P*, 1400mm; *R*, 780 mm; *E*, 620mm) are humid. The amplitude of the water storage variations between years were 7, 37.2 and 65 mm for the three rivers respectively, one magnitude order smaller than fluxes of *P*, *R* and *E*. Although the observations cannot be directly extrapolated to other regions, the possibility seems remote that the use of a 7-year aggregated time strongly violates the assumption of the steady state condition.

Mathematically, the LI method is unrelated to a functional form and applies to communities other than just hydrology. For example, identifying the carbon emission budgets (an allowable amount of anthropogenic CO_2 emission consistent with a limiting warming target), is crucial for global efforts to mitigate climate change. The LI method suggested that the emission budgets depends on both the emission magnitude and pathway (timing of emissions), in line with a recent study by Gasser *et al.* (2018). Hence, an optimal pathway would bring about an elevated carbon budget unless the carbon-climate system behaves in a linear fashion. This study presented the LI method using time-series data, but it applies equally to the case of spatial series of data. Given a model that relates fluvial or aeolian sediment load to the influencing factors (e.g. rainfall and topography), for example, the LI method can be used to separate their contributions to the sediment-load change along a river or in the along-wind direction

5 Conclusions

Based on the line integral, I found a mathematically precise solution to partition the effects of a number of independent variables on the change in the dependent variable. I then applied the method to partition the effects on runoff of climatic and catchment conditions within the Budyko framework. The method reveals that in addition to the change magnitude, the change pathways of climatic and catchment conditions also exert control on their impacts on runoff. Instead of using the runoff sensitivity at a point, the LI method uses the path-averaged sensitivity, thereby ensuring a mathematically precise partition. I further examined the spatiotemporal variability of the path-averaged sensitivity. Time-wise the runoff sensitivity is stable to climate but highly variable to catchment properties, suggesting that it is reliable to predict future climate effects using earlier observations but care must be taken when predicting the catchment effects. Space-wise (between catchments) the runoff sensitivity was highly variable both to climatic and catchment conditions, but it can be well depicted by the long-term means of the climatic and catchment conditions. As a mathematically accurate scheme, the LI method has the potential to be a generic attribution approach in the environmental sciences.

Data availability

The data used in this study are freely available by contacting the authors.

Author contribution

MZ designed the study, analyzing the data and wrote the manuscript.

Competing interests

The authors declare that they have no conflict of interest.

Appendix A: Derivation of equation $\Delta z = \int_L f_x(x,y)dx + \int_L f_y(x,y)dy$

We define that the curve L in Fig. 1(c) is given by a parametric equation: $x = x(t)$, $y = y(t)$, $t \in [t_0, t_N]$, then $\Delta z = z_N - z_0 = f[x(t_N), y(t_N)] - f[x(t_0), y(t_0)]$. Substituting the parametric equations, we get:

The right-hand side of the equation = $\int_{t_0}^{t_N} f_x[x(t), y(t)]dx(t) + \int_{t_0}^{t_N} f_y[x(t), y(t)]dy(t)$

$$= \int_{t_0}^{t_N} \left\{ f_x[x(t), y(t)]x'(t) + f_y[x(t), y(t)]y'(t) \right\} dt \qquad \text{(A1)}$$

Let $g(t) = f[x(t), y(t)]$, and after using the chain rule to differentiate g with respect to t, we obtain:

$$g'(t) = \frac{\partial g}{\partial x}\frac{dx}{dt} + \frac{\partial g}{\partial y}\frac{dy}{dt} = f_x[x(t), y(t)]x'(t) + f_y[x(t), y(t)]y'(t) \qquad \text{(A2)}$$

It shows that $g'(t)$ is just the integrand in Eq. (A1), Eq. (A1) can then be rewritten as:

The right-hand side of the equation $= \int_{t_0}^{t_N} g'(t)\,\mathrm{d}t = [g(t)]_{t_0}^{t_N} = g(t_N) - g(t_0)$ $= f[x(t_N), y(t_N)] - f[x(t_0), y(t_0)] =$ The left-hand side of the equation

Appendix B: The sum of $\int_L f_x(x,y)dx$ and $\int_L f_y(x,y)dy$ is path independent

Theorem: Given an open simply-connected region G (i.e., no holes in G) and two functions $P(x, y)$ and $Q(x, y)$ that have continuous first-order derivatives, if and only if $\partial P / \partial y = \partial Q / \partial x$ throughout G, then $\int_L P(x,y)dx + \int_L Q(x,y)dy$ is path independent, i.e., it depends solely on the starting and ending point of L.

We have $\partial f_x / \partial y = \partial^2 z / \partial x \partial y$ and $\partial f_y / \partial x = \partial^2 z / \partial y \partial x$. As $\partial^2 z / \partial x \partial y = \partial^2 z / \partial y \partial x$, we can state that $\partial f_x / \partial y = \partial f_y / \partial x$, meeting the above condition and proving that $\int_L f_x(x,y)dx + \int_L f_y(x,y)dy$ is path independent. The statement was further exemplified using a fictitious example in Appendix C.

Appendix C: A fictitious example to show how the LI method works

It is assumed that runoff (R, mm yr^{-1}) at a site increases from 120 to 195 mm yr^{-1} with ΔR = 75 mm yr^{-1}; meanwhile, precipitation (P, mm yr^{-1}) varies from 600 to 650 mm yr^{-1} (ΔP = 75 mm yr^{-1}) and runoff coefficient (C_R, dimensionless) from 0.2 to 0.3 (ΔC_R = 0.1). The goal is to partition ΔR into the effects of precipitation (ΔR_P) and runoff coefficient (ΔR_{C_R}) provided that P and C_R are independent. We have a function $R = PC_R$ and its partial derivatives $\partial R / \partial P = C_R$ and $\partial R / \partial C_R = P$. Given a path L along which P and C_R change and using Eq. (3), the LI method evaluates ΔR_P and ΔR_{C_R} as:

$$\Delta R_{C_R} = \int_L \partial R / \partial C_R dC_R = \int_L P dC_R \quad \text{and} \quad \Delta R_P = \int_L \partial R / \partial P dP = \int_L C_R dP \qquad \text{(C1)}$$

The result differs depending on L but the sum of ΔR_P and ΔR_{C_R} uniformly equals ΔR. It will be demonstrated using Fig. 1(c), in which the x-axis represents C_R and the y-axis P. Point A denotes the initial state (C_R = 0.2, P = 600) and point C the terminal state (C_R = 0.3, P = 650). I calculated ΔR_P and ΔR_{C_R} along three fictitious paths as follows:

1) L=AC. Line segment AC has equation $P = 500C_R + 500$, $0.2 \le C_R \le 0.3$. Let's take C_R as the parameter and write the equation in the parametric form as $P = 500C_R + 500$, $C_R = C_R$, $0.2 \le C_R \le 0.3$. By substituting the equation into Eq. (C1), we have:

$$\Delta R_{C_R} = \int_{AC} P dC_R = \int_{0.2}^{0.3} (500C_R + 500) dC_R = 62.5$$

$$\Delta R_P = \int_{AC} C_R dP = \int_{AC} C_R d(500C_R + 500) = 500 \int_{0.2}^{0.3} C_R dC_R = 12.5$$

2) L=AB+BC. To evaluate on the broken line, we can evaluate separately on AB and BC and then sum them up. The equation for AB is P = 600, $0.2 \le C_R \le 0.3$, and is C_R = 0.3, $600 \le P \le 650$ for BC. Notes that a constant C_R or P implies that dC_R = 0 or dP = 0. Eq. (C1) then becomes:

$$\Delta R_{C_R} = \int_{AB+BC} P dC_R = \int_{AB} P dC_R + \int_{BC} P dC_R = \int_{0.2}^{0.3} 600 dC_R + 0 = 60$$

$$\Delta R_P = \int_{AB+BC} C_R dP = \int_{AB} C_R dP + \int_{BC} C_R dP = 0 + \int_{600}^{650} 0.3 dP = 15$$

3) L=AD+DC. The equation for AD is C_R = 0.2, $600 \le P \le 650$ and is P = 650, $0.2 \le C_R \le 0.3$ for DC. ΔR_P and ΔR_{C_R} are evaluated as:

$$\Delta R_{C_R} = \int_{AD+DC} P dC_R = \int_{AD} P dC_R + \int_{DC} P dC_R = 0 + \int_{0.2}^{0.3} 650 dC_R = 65$$

$$\Delta R_P = \int_{AD+DC} C_R dP = \int_{AD} C_R dP + \int_{DC} C_R dP = \int_{600}^{650} 0.2dP + 0 = 10$$

As we expect, the sum of ΔR_P and ΔR_{CR} persistently equals ΔR although ΔR_P and ΔR_{CR} varies with L.

Appendix D: Derivation of $\Delta R = \overline{\lambda_P}\Delta P + \overline{\lambda_{E_0}}\Delta E_0 + \overline{\lambda_n}\Delta n$

If we partition the interval $[x_0, x_N]$ in Fig. 1(c) into N distinct bins of the same width $\Delta x_{\mathrm{i}} = \Delta x/N$. Eq. (3a) can then be rewritten as:

$$\Delta Z_x = \int_L f_x(x, y)dx = \lim_{\tau\to 0}\sum_{i=0}^{N-1} f_x(x_i, y_i)\Delta x_i = \lim_{\tau\to 0} N\Delta x_i \frac{\sum_{i=0}^{N-1} f_x(x_i, y_i)}{N} = \Delta x \lim_{\tau\to 0}\frac{\sum_{i=0}^{N-1} f_x(x_i, y_i)}{N} = \overline{\lambda_x}\Delta x$$

where $\overline{\lambda_x} = \lim_{\tau\to 0}\frac{\sum_{i=1}^{N} f_x(x_i, y_i)}{N}$, denoting the average of $f_{\mathrm{x}}(x, y)$ along the curve L. Likewise, we have $\Delta Z_y = \overline{\lambda_y}\Delta y$, where $\overline{\lambda_y}$ denotes the average of $f_{\mathrm{y}}(x, y)$ along the curve L. As a result, we have:

$$\Delta Z = \overline{\lambda_x}\Delta x + \overline{\lambda_y}\Delta y \qquad \text{(D1)}$$

The result can readily be extended to a function of three variables. Applying the mathematic derivation above to the MCY Equation results in a precise form of Eq. (7):

$$\Delta R = \Delta R_P + \Delta R_{E_0} + \Delta R_n = \overline{\lambda_P}\Delta P + \overline{\lambda_{E_0}}\Delta E_0 + \overline{\lambda_n}\Delta n, \qquad \text{(D2)}$$

where $\Delta R_P = \overline{\lambda_P}\Delta P$, $\Delta R_{E_0} = \overline{\lambda_{E_0}}\Delta E_0$, $\Delta R_n = \overline{\lambda_n}\Delta n$, and $\overline{\lambda_P}$, $\overline{\lambda_{E_0}}$ and $\overline{\lambda_n}$ denote the arithmetic mean of $\partial R/\partial P$, $\partial R/\partial E_0$, and $\partial R/\partial n$ along a path of climate and catchment changes, respectively. Because $\overline{\lambda_P} = \Delta R_P/\Delta P$, $\overline{\lambda_{E_0}} = \Delta R_{E_0}/\Delta E_0$, and $\overline{\lambda_n} = \Delta R_n/\Delta n$, $\overline{\lambda_P}$, $\overline{\lambda_{E_0}}$ and $\overline{\lambda_n}$ also implies the runoff change due to a unit change in P, E_0 and n, respectively.

Acknowledgments

This work was funded by the National Natural Science Foundation of China (41671278), the GDAS' Project of Science and Technology Development (2019GDASYL-0103043) and (2019GDASYL-0502004). I thank Mr. Y.Q. Zheng for his assistance with the mathematic derivations.

References

Barnett, T. P., Pierce, D. W., Hidalgo, H. G., Bonfils, C., Santer, B. D., Das, T., .Bala G., Woods, A. W., Nozawa, T., Mirin, A. A., Cayan D. R., and M. D. Dettinger: Human-induced changes in the hydrology of the western United States. Science, 319(5866), 1080-1083. https://doi.org/10.1126/science.1152538, 2008.

Berghuijs, W. R., R. A. Woods: Correspondence: Space-time asymmetry undermines water yield assessment. Nature Communications 7, 11603. https://doi.org/ 10.1038/ncomms11603, 2016.

Binley, A. M., Beven, K. J., Calver, A., and L. G. Watts: Changing responses in hydrology: assessing the uncertainty in physically based model predictions. Water Resources Research, 27(6), 1253-1261. https://doi.org/10.1029/91WR00130, 1991.
Brown, A. E., Zhang, L., McMahon, T. A., Western, A. W. and R. A Vertessy: A review of paired catchment studies for determining changes in water yield resulting from alterations in vegetation. Journal of Hydrology, 310, 26–61. https://doi.org/ 10.1016/j.jhydrol.2004.12.010, 2005.
Budyko, M. I.: Climate and Life. Academic, N. Y. 1974.
Carmona, A. M., Sivapalan, M., Yaeger, M. A., and Poveda, G.: Regional patterns of interannual variability of catchment water balances across the continental US: A Budyko framework. Water Resources Research, 50, 9177–9193. https://doi:10.1002/2014wr016013, 2014.
Choudhury, B. J.: Evaluation of an empirical equation for annual evaporation using field observations and results from a biophysical model. Journal of Hydrology, 216, 99–110. https://doi.org/10.1016/S0022-1694(98)00293-5, 1999.
Dey, P., and A. Mishra: Separating the impacts of climate change and human activities on streamflow: A review of methodologies and critical assumptions. Journal of Hydrology, 548, 278-290. https://doi.org/10.1016/j.jhydrol.2017.03.014, 2017.
Donohue, R. J., M. L. Roderick, and T. R. McVicar: On the importance of including vegetation dynamics in Budyko's hydrological model. Hydrology and Earth System Sciences, 11, 983–995. https://doi.org/10.5194/hess-11-983-2007, 2007.
Gao, G., Ma, Y., and B. Fu: Multi-temporal scale changes of streamflow and sediment load in a loess hilly watershed of China. Hydrological Processes, 30(3), 365-382, 10.1002/hyp.10585, 2016.
Gasser, T., M. Kechiar, P. Ciais, E. J. Burke, T. Kleinen, D. Zhu, Y. Huang, A. Ekici, and M. Obersteiner: Path-dependent reductions in CO_2 emission budgets caused by permafrost carbon release. Nature Geoscience, 11, 830–835. https://doi.org/ 10.1038/s41561-018-0227-0, 2018.
Jiang, C., Xiong, L., Wang, D., Liu, P., Guo, S., and Xu C.: Separating the impacts of climate change and human activities on runoff using the Budyko-type equations with time-varying parameters. Journal of Hydrology, 522, 326-338, 10.1016/j.jhydrol.2014.12.060, 2015.
Li, Z., Ning, T., Li, J., and D. Yang: Spatiotemporal variation in the attribution of streamflow changes in a catchment on China's Loess Plateau. Catena, 158:1–8. https://doi.org/10.1016/j.catena.2017.06.008, 2017.
Liang, W., D. Bai, F. Wang, B. Fu, J. Yan, S. Wang, Y. Yang, D. Long, and M. Feng: Quantifying the impacts of climate change and ecological restoration on streamflow changes based on a Budyko hydrological model in China's Loess Plateau. Water Resources Research, 51, 6500–6519. https://doi.org/10.1002/ 2014WR016589, 2015.
Liu, J., Zhang, Q., Singh, V. P., and P. Shi. Contribution of multiple climatic variables and human activities to streamflow changes across China. Journal of Hydrology, 545, 145-162. https://doi.org/10.1016/j.jhydrol.2016.12.016, 2016.
Mezentsev, V. S.: More on the calculation of average total evaporation. Meteorol. Gidrol., 5, 24–26, 1955.
Ning, T., Li, Z., and W. Liu: Vegetation dynamics and climate seasonality jointly control the interannual catchment water balance in the Loess Plateau under the Budyko framework, Hydrology and Earth System Sciences, 21, 1515-1526. https://doi.org/10.5194/hess-2016-484, 2017.

Roderick, M. L., and G. D. Farquhar: A simple framework for relating variations in runoff to variations inclimatic conditions and catchment properties. Water Resources Research, 47, W00G07, https://doi.org/10.1029/2010WR009826, 2011.

Sankarasubramanian, A., R. M. Vogel, and J. F. Limbrunner: Climate elasticity of streamflow in the United States. Water Resources Research, 37(6), 1771-1781. https://doi.org/10.1029/2000WR900330, 2001.

Schaake, J. C.: From climate to flow. Climate Change and U.S. Water Resources, edited by P. E. Waggoner, chap. 8, pp. 177 – 206, John Wiley, N. Y. 1990.

Sivapalan, M., Yaeger, M. A., Harman, C. J., Xu, X. Y., and P. A. Troch: Functional model of water balance variability at the catchment scale: 1. Evidence of hydrologic similarity and space-time symmetry, Water Resources Research, 47, W02522, doi:10.1029/2010wr009568, 2011.

Sposito, G.: Understanding the Budyko equation. Water, 9(4), 236. https://doi.org/10.3390/w9040236, 2017.

Sun, Y., Tian, F., Yang, L., and H. Hu: Exploring the spatial variability of contributions from climate variation and change in catchment properties to streamflow decrease in a mesoscale basin by three different methods. Journal of Hydrology, 508(2), 170-180, https://doi.org/10.1016/j.jhydrol.2013.11.004, 2014.

Wang, D., and M. Hejazi: Quantifying the relative contribution of the climate and direct human impacts on mean annual streamflow in the contiguous United States. Water Resources Research, 47, W00J12, https://doi.org/10.1029/2010WR010283, 2011.

Wang, W., Q. Shao, T. Yang, S. Peng, W. Xing, F. Sun, and Y. Luo: Quantitative assessment of the impact of climate variability and human activities on runoff changes: A case study in four catchments of the Haihe River basin, China. Hydrological Processes, 27(8), 1158–1174. https://doi.org/10.1002/hyp.9299, 2013.

Wu, J., Miao, C., Wang, Y., Duan, Q., and X. Zhang: Contribution analysis of the long-term changes in seasonal runoff on the Loess Plateau, China, using eight Budyko-based methods. Journal of hydrology, 545, 263-275. https://doi.org/10.1016/j.jhydrol.2016.12.050, 2017a.

Wu, J., Miao, C., Zhang, X., Yang, T., and Q. Duan: Detecting the quantitative hydrological response to changes in climate and human activities. Science of the Total Environment, 586, 328-337. https://doi.org/10.1016/j.scitotenv.2017.02.010, 2017b.

Xu, X., Yang, D., Yang, H. and Lei, H.: Attribution analysis based on the Budyko hypothesis for detecting the dominant cause of runoff decline in Haihe basin. Journal of Hydrology, 510: 530-540. http://dx.doi.org/10.1016/j.jhydrol.2013.12.052, 2014.

Yang, H., D. Yang, Z. Lei, and F. Sun: New analytical derivation of the mean annual water-energy balance equation. Water Resources Research, 44, W03410. https://doi.org/10.1029/2007WR006135, 2008.

Yang, H., and D. Yang: Derivation of climate elasticity of runoff to assess the effects of climate change on annual runoff. Water Resources Research, 47, W07526. https://doi.org/10.1029/2010WR009287, 2011.

Yang, H., D. Yang, and Q. Hu: An error analysis of the Budyko hypothesis for assessing the contribution of climate change to runoff. Water Resources Research, 50, 9620–9629. https://doi.org/10.1002/ 2014WR015451, 2014.

Zhao, Q. L., Liu, X. L., Ditmar, P., Siemes, C., Revtova, E., Hashemi-Farahani, H., and R. Klees: Water storage variations of the Yangtze, Yellow, and Zhujiang river basins derived from the DEOS Mass Transport (DMT-1) model. Science China-Earth Sciences, 54, 667-677. https://doi.org/10.1007/s11430-010-4096-7, 2011.

Zhang, S., H. Yang, D. Yang, and A. W. Jayawardena: Quantifying the effect of vegetation change on the regional water balance within the Budyko framework. Geophysical Research Letters, 43, 1140–1148. https://doi.org/10.1002/2015GL066952, 2016.

Zhang, L., Dawes, W. R. and G. R. Walker: Response of mean annual evapotranspiration to vegetation changes at catchment scale. Water Resources Research 37, 701–708. doi; 10.1029/2000WR900325, 2001.

Zhang, L., F. Zhao, A. Brown, Y. Chen, A. Davidson, and R. Dixon: Estimating Impact of Plantation Expansions on Streamflow Regime and Water Allocation. CSIRO Water for a Healthy Country, Canberra, Australia. 2010.

Zhang, L., F. Zhao, Y. Chen, and R. N. M. Dixon: Estimating effects of plantation expansion and climate variability on streamflow for catchments in Australia. Water Resources Research, 47, W12539, https://doi.org/10.1029/2011WR010711, 2011.

Zheng, H., L. Zhang, R. Zhu, C. Liu, Y. Sato, and Y. Fukushima: Responses of streamflow to climate and land surface change in the headwaters of the Yellow River Basin. Water Resources Research, 45, W00A19. https://doi.org/10.1029/2007WR006665, 2009.

Zhou, S., B. Yu, L. Zhang, Y. Huang, M. Pan, and G. Wang (2016), A new method to partition climate and catchment effect on the mean annual runoff based on the Budyko complementary relationship. Water Resources Research, 52, 7163–7177. https://doi.org/10.1002/2016WR019046, 2016.

Table 1. Summary of the long-term hydrometeorological characteristics of the selected catchments[a]

Catchment No.[b]	Area (km^2)	R	P	E_0	n	AI	Reference Period	Evaluation Period	The Last Subperiod
1	391	218	1014	935	3.5	0.92	1933-1955	1956-2008	1998-2008
2	16.64	32.9	634	1087	3.16	1.71	1979-1984	1985-2008	1999-2008
3	559	183	787	780	2.68	0.99	1960-1978	1979-2000	1993-2000
4	606	73	729	998	3.07	1.37	1971-1995	1996-2009	2003-2009
5	760	77.9	689	997	2.66	1.45	1970-1995	1996-2009	2003-2009
6	502	57.2	730	988	3.59	1.35	1974-1995	***1996-2008***	***1996-2008***
7	673	431	1013	953	1.34	0.94	1947-1955	1956-2008	1998-2008
8	390	139	840	1021	2.61	1.22	1966-1980	1981-2005	1995-2005
9	1130	20.7	633	1077	3.79	1.7	1972-1982	1983-2007	1997-2007
10	3.2	37.5	631	954	3.49	1.51	1989-1991	1992-2009	1999-2009
11	1.95	111	767	901	3.06	1.18	1990-1992	***1993-2005***	***1993-2005***
12	89	272	963	826	2.82	0.86	1958-1965	1966-1999	1987-1999
13	243	38.5	735	1010	4.27	1.37	1989-1995	***1996-2007***	***1996-2007***
14	56.35	65.8	744	1007	3.35	1.35	1989-1995	***1996-2008***	***1996-2008***
15	14484	385	893	1022	1.11	1.14	1970-1989	***1990-2000***	***1990-2000***
16	38625	461	985	1087	1.03	1.1	1970-1989	***1990-2000***	***1990-2000***
17	59115	388	897	1161	1.02	1.29	1970-1989	***1990-2000***	***1990-2000***
18	95217	371	881	1169	1.03	1.33	1970-1989	***1990-2000***	***1990-2000***
19	121,972	171	507	768	1.17	1.52	1960-1990	***1991-2000***	***1991-2000***
20	106,500	60.5	535	905	2.25	1.69	1960-1970	1971-2009	1999-2009
21	5891	34.4	506	964	2.54	1.91	1952-1996	1997-2011	2004-2011

[a]R, P, and E_0 represents mean annual runoff, precipitation and potential evaporation, all in mm yr^{-1}. n (dimensionless) is the parameter representing catchment properties in the MCY equation. AI is dimensionless aridity index ($AI = E_0/P$). Data of Catchments 1-14 were derived from Zhang *et al.* (2010). Data of Catchments 15-18 were from Sun *et al.* (2014). Data of Catchments 19-21 were from Zheng *et al.* (2009), Jiang *et al.* (2015), and Gao *et al.* (2016), respectively. I used the change points given in the literatures to divide the observation period into the reference and elevation periods. The LI method further divides the evaluation period into a number of subperiods. The column "The Last Subperiod" denotes the last one, which was used as the evaluation period for the total differential method, the decomposition method and the complementary method. The bold and italic rows denote that the column "Evaluation Period" is the same as the column "The Last Subperiod".

[b]Catchments 1-14 are in Ausralia and the others in China. 1: Adjungbilly CK; 2: Batalling Ck; 3: Bombala River; 4: Crawford River; 5: Darlot Ck; 6: Eumeralla River; 7: Goobarragandra CK; 8: Jingellic CK; 9: Mosquito CK; 10: Pine Ck; 11: Red Hill; 12: Traralgon Ck; 13: Upper Denmark River; 14: Yate Flat Ck; 15: Yangxian station, Hang River; 16: Ankang station, Hang River; 17: Baihe station, Hang River; 18: Danjiangkou station, Hang River; 19: Headwaters of the Yellow River Basin; 20: Wei River; 21: Yan River.

Table 2. Comparisons of R (mm yr^{-1}), P (mm yr^{-1}), E_0 (mm yr^{-1}), and n (dimensionless) between the reference and the evaluation periods[a]

Catchment No.	R_1	R_2	P_1	P_2	E_{01}	E_{02}	n_1	n_2	ΔR	ΔP	ΔE_0	Δn
1	223	216	959	1038	950	928	2.7	4.1	-7.2	79.2	-21	1.4
2	40.6	31	655	629	1087	1087	3	3.2	-9.7	-27	0	0.2
3	249	127	847	736	780	780	2.3	3.2	-122	-112	0.4	0.9
4	90.6	41.5	753	685	1002	989	2.9	3.7	-49	-67	-13	0.8
5	94.9	46.3	718	633	1000	992	2.5	3	-49	-85	-9	0.5
6	70.8	34.3	756	687	989	987	3.4	4.1	-36	-69	-2	0.6
7	575	406	1123	995	931	957	1.1	1.4	-169	-128	25	0.3
8	139	139	871	821	1043	1008	2.7	2.5	-0.4	-50	-35	0
9	24.1	19.2	659	621	1100	1067	3.7	3.8	-4.9	-37	-33	0.1
10	116	24.3	588	638	927	958	1.7	4.2	-92	50.4	31	2.5
11	297	68	986	716	884	905	2.3	3.6	-229	-271	22	1.3
12	301	265	992	956	820	828	2.7	2.8	-36	-36	7.4	0.1
13	48.5	32.6	752	725	991	1021	4.2	4.4	-16	-28	30	0.2
14	90.4	52.6	753	739	991	1015	2.9	3.7	-38	-14	24	0.8
15	435	295	948	795	1008	1047	1.1	1.2	-139	-153	38	0.1
16	520	353	1035	894	1074	1109	1	1.2	-167	-141	35	0.2
17	441	291	939	820	1149	1182	1	1.2	-151	-119	33	0.2
18	412	296	913	821	1163	1179	1	1.1	-116	-92	15	0.2
19	180	144	512	491	774	751	1.1	1.3	-36	-21	-23	0.2
20	90.2	52.1	585	520	895	908	2.1	2.3	-38	-65	13	0.2
21	37.7	24.6	521	462	954	995	2.6	2.5	-13	-59	41	0

[a]The subscript "1" denotes the reference period and "2" denotes the evaluation period. $\Delta X = X_2 - X_1$ (X as a substitute for R, P, E_0, and n).

Table 3. Effects of precipitation (ΔR_P, mm yr^{-1}), potential evapotranspiration (ΔR_{E_0}, mm yr^{-1}), and catchment changes (ΔR_n, mm yr^{-1}) on the mean annual runoff resulting from the four methods

Catchment NO.[a]	LI Method			Decomposition Method	Total Differential Method			Complementary Method		
	ΔR_P	ΔR_{E_0}	ΔR_n	ΔR_n	ΔR_P	ΔR_{E_0}	ΔR_n	ΔR_P	ΔR_{E_0}	ΔR_n
1	-70.9	-8.99	-24.3	-44.6	-67	4.82	-62	-60.7	4.34	-47.3
2	-6.49	0.95	-9.74	-9.65	-7.2	1.3	-13	-6.23	1.13	-10.2
3	-89	25.9	-140	-128	-104	26.6	-483	-88	25.7	-140
4	-18.1	2.09	-35.4	-36.3	-18	2.37	-58	-14.8	1.99	-38.5
5	-27.9	1.14	-21.3	-18.6	-34	1.18	-27	-28.1	0.97	-20.9
6	-19.9	0.29	-16.7	-14.9	-24	0.36	-22	-19.9	0.29	-16.7
7	-211	-7.19	-101	-90.9	-236	-6.9	-134	-211	-6.21	-102
8	-32.2	12.3	-14.4	-12.6	-35	12.6	-15	-32.9	11.9	-13.3
9	-11.8	3.02	-9.96	-8.45	-13	0.85	-20	-8.76	0.56	-10.5
10	19.47	-5.61	-119	-96.5	0.91	-10	-291	0.56	-6.53	-99.1
11	-150	-7.46	-71.8	-60.7	-188	-9.4	-113	-144	-7.04	-78.3
12	-9.88	-3.99	-79.2	-82	-11	-0.5	-154	-10.8	-0.57	-81.6
13	-6.98	-4.36	-4.54	-4.21	-8	-5.1	-5.2	-7	-4.38	-4.51
14	-4.84	-4.42	-28.7	-27.9	-5.6	-5	-37	-4.85	-4.4	-28.6
15	-104	-8.56	-24.8	-23	-110	-9.4	-27	-103	-8.52	-25.1
16	-99.3	-7.99	-58.8	-56	-105	-8.3	-68	-99	-7.92	-59.1
17	-78.8	-6.26	-63.9	-61	-84	-6.5	-76	-78.6	-6.2	-64.2
18	-60.1	-2.79	-53.5	-52	-64	-2.9	-62	-60	-2.77	-53.6
19	-11.9	3.89	-27.6	-27	-12	3.81	-31	-11.9	3.85	-27.5
20	-27.5	-2.46	-18.5	-17	-31	-4.4	-26	-25.5	-3.47	-19.5
21	-10.4	-3.47	-2.11	-3.4	-9.9	-4.8	-4.8	-8.27	-3.86	-3.82

[a]The bold and italic numbers denote that the evaluation period comprises a single subperiod.

Table 4. Comparisons of the path-averaged with the point sensitivities of runoff [a, b]

Catchment NO.	$\overline{\lambda_P}$	$\overline{\lambda_{E0}}$	$\overline{\lambda_n}$	λ_{Pf}	λ_{E0f}	λ_{nf}	λ_{Pb}	λ_{E0b}	λ_{nb}
1	0.68	-0.55	-17	0.621	-0.39	-71.8	0.497	-0.32	-39.7
2	0.2	-0.08	-27.3	0.227	-0.1	-30.9	0.168	-0.07	-19.6
3	0.58	-0.36	-26.7	0.68	-0.42	-79	0.473	-0.39	-6.29
4	0.3	-0.16	-30.5	0.39	-0.2	-50.1	0.248	-0.14	-21
5	0.33	-0.14	-43.1	0.394	-0.19	-59.4	0.264	-0.12	-33.2
6	0.29	-0.16	-26.5	0.352	-0.2	-34.9	0.228	-0.12	-19.1
7	0.71	-0.32	-223	0.781	-0.33	-299	0.615	-0.26	-157
8	0.49	-0.26	-77.9	0.478	-0.27	-64.9	0.429	-0.24	-50.7
9	0.16	-0.07	-11.8	0.161	-0.07	-17.6	0.052	-0.02	-4.31
10	0.27	-0.12	-40.9	0.45	-0.16	-99.9	0.101	-0.05	-7.8
11	0.55	-0.35	-56.1	0.695	-0.44	-88.2	0.367	-0.22	-30.7
12	0.72	-0.45	-57.3	0.74	-0.53	-61.1	0.775	-0.67	-16.7
13	0.25	-0.15	-19.8	0.29	-0.17	-22.5	0.219	-0.12	-17.1
14	0.34	-0.18	-37.2	0.393	-0.21	-48.6	0.291	-0.16	-27.8
15	0.68	-0.22	-275	0.719	-0.25	-303	0.635	-0.2	-246
16	0.7	-0.23	-326	0.745	-0.24	-378	0.659	-0.21	-279
17	0.66	-0.19	-320	0.708	-0.2	-378	0.609	-0.18	-267
18	0.65	-0.19	-315	0.692	-0.19	-363	0.614	-0.18	-270
19	0.58	-0.17	-153	0.602	-0.17	-175	0.552	-0.17	-134
20	0.32	-0.12	-50.1	0.402	-0.16	-69.6	0.255	-0.1	-37.7
21	0.2	-0.06	-29.2	0.234	-0.09	-34	0.157	-0.05	-22.6

[a] $\overline{\lambda_P}$ (mm mm^{-1}), $\overline{\lambda_{E0}}$ (mm mm^{-1}), and $\overline{\lambda_n}$ (dimensionless) represent the path-averaged sensitivities of runoff to precipitation, potential evaporation, and catchment properties (see Appendix D). If the evaluation period comprises only one subperiod, $\overline{\lambda_P}$, $\overline{\lambda_{E0}}$ and $\overline{\lambda_n}$ was calculated as: $\overline{\lambda_P} = \Delta R_P / \Delta P$, $\overline{\lambda_{E0}} = \Delta R_{E0} / \Delta E_0$,and $\overline{\lambda_n} = \Delta R_n / \Delta n$. If the evaluation period comprises N>1 subperiods, the equations become: $\overline{\lambda_P} = \sum_{i=1}^{N} |\Delta R_{Pi}| / \sum_{i=1}^{N} |\Delta P_i|$, $\overline{\lambda_{E0}} = -\sum_{i=1}^{N} |\Delta R_{E0i}| / \sum_{i=1}^{N} |\Delta E0_i|$, and $\overline{\lambda_n} = -\sum_{i=1}^{N} |\Delta R_{ni}| / \sum_{i=1}^{N} |\Delta n_i|$, where the subscript i denotes the ith subperiod.

[b] λ_P , λ_{E0} , and λ_n represent the point sensitivities of runoff . The subscript "*f*" represents a forward approximation, i.e. substituting the observed mean annual values of the reference period into Eq. (2) to calculate the sensitivities, while the subscript "*b*" represents a backward approximation, i.e. substituting the observed mean annual values of the evaluation period into Eq. (2).

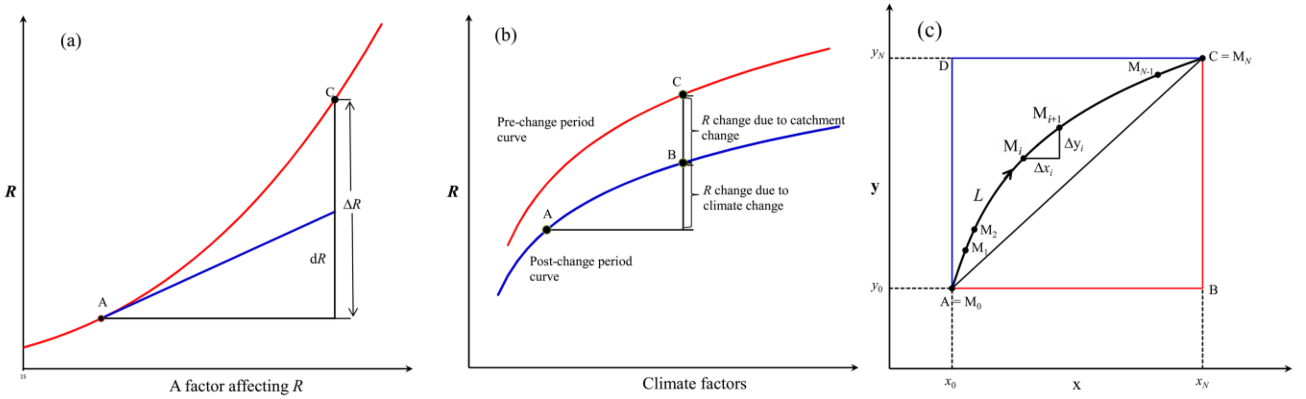

Fig. 1. A schematic plot to illustrate (a) the total differential method, (b) the decomposition method, and (c) the LI method. Pont A denotes the initial state and Point C the terminal state. Notes that unlike (a) and (b), the y-axis is not *R* in (c).

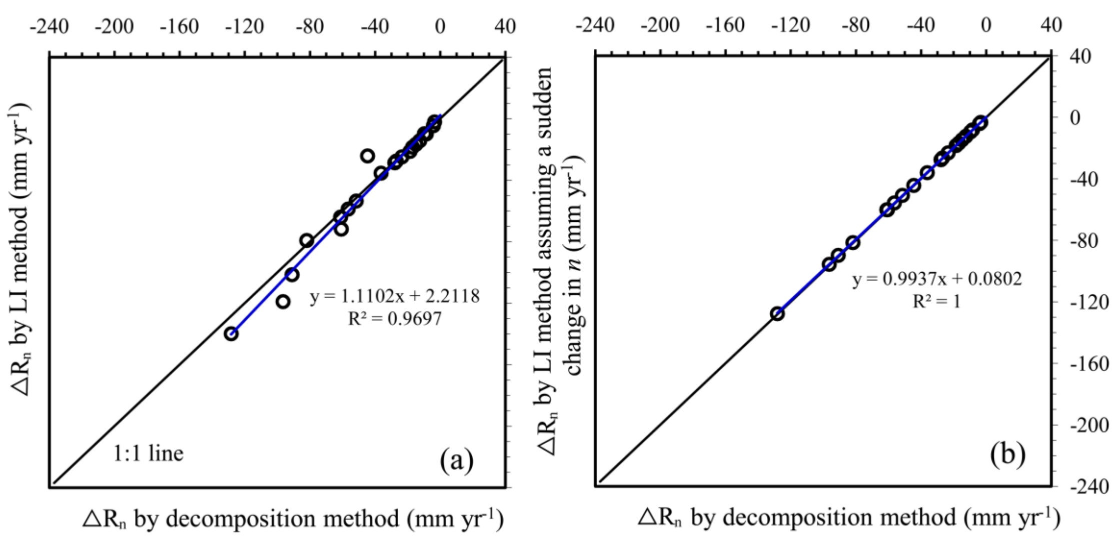

Fig. 2. Comparison between the LI method and the decomposition method. (a) Comparison of the estimated contribution to the runoff change from catchment change (ΔR_n); (b) the decomposition method is equivalent to the LI method that assumes a sudden change in catchment properties following climate change. In this case, the integral path of the LI method is the broken line AB+BC in Fig. 1(c) (*x* represents climate factors and *y* catchment properties, *i.e.* *n*) and $\Delta R_n = \int_{AB+BC} \frac{\partial R}{\partial n} dn = \int_{AB} \frac{\partial R}{\partial n} dn + \int_{BC} \frac{\partial R}{\partial n} dn = 0 + \int_{BC} \frac{\partial R}{\partial n} dn = \int_{n_1}^{n_2} f_n(P_2, E_{02}, n) dn$, where the subscript "1" denotes the reference period and "2" denotes the last subperiod of the evaluation period.

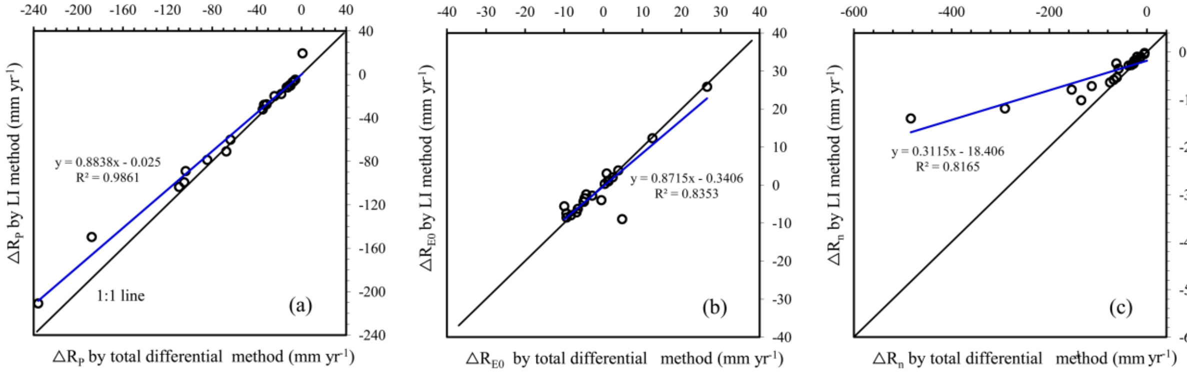

Fig. 3. Comparison of the estimated contribution to runoff from the changes in (a) precipitation (ΔR_P), (b) potential evapotranspiration (ΔR_{E_0}), and (c) catchment properties (ΔR_n) between the LI method and the total differential method.

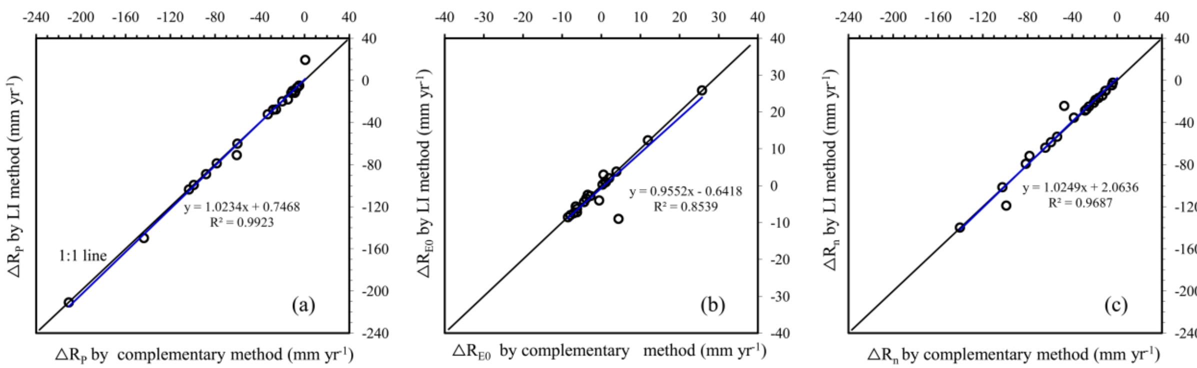

Fig. 4. Comparison of (a) ΔR_P, (b) ΔR_{E_0}, and (c) ΔR_n between the LI method and the complementary method (a = 0.5).

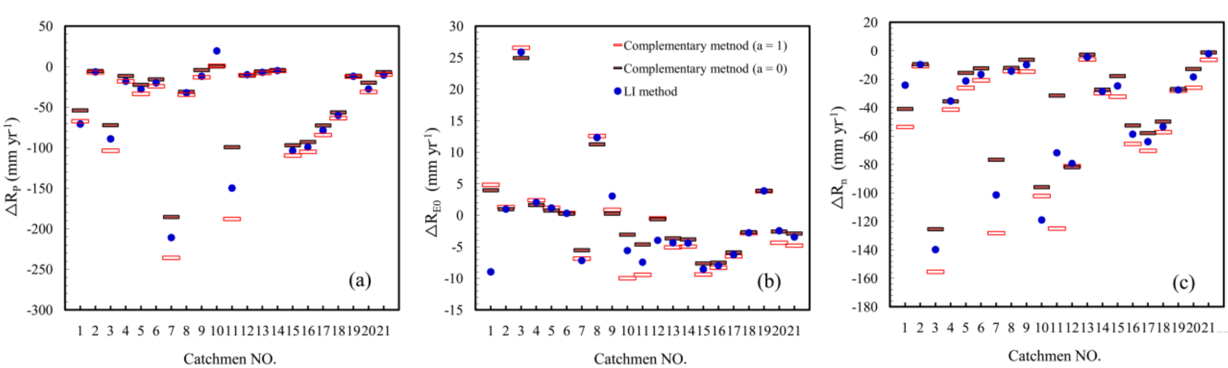

Fig. 5. Comparison of (a) ΔR_P, (b) ΔR_{E_0}, and (c) ΔR_n by the LI method with the upper (a=1) and lower (a=0) bounds given by the complementary method. According to Zhou *et al*. (2016), the upper and lower bounds of ΔR_P, ΔR_{E_0}, and ΔR_n are reached when a is 0 or 1.

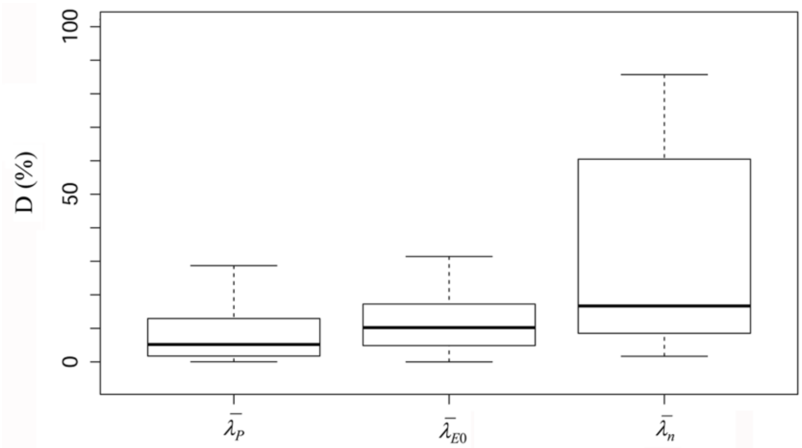

Fig. 6. Boxplots showing the temporal variability of the path-averaged sensitivities of water yield to precipitation ($\overline{\lambda_P}$), potential evapotranspiration ($\overline{\lambda_{E0}}$), and catchment properties ($\overline{\lambda_n}$). D (%) was calculated as the relative difference between the sensitivity of the whole evaluation period and that of a subperiod. In the calculations, I excluded the catchments whose evaluation periods were not long enough to comprise two or more subperiods. Box spans the inter-quartile range (IQR) and solid lines are medians. Whiskers represent data range, excluding statistical outliers, which extend more than 1.5IQR from the box ends.

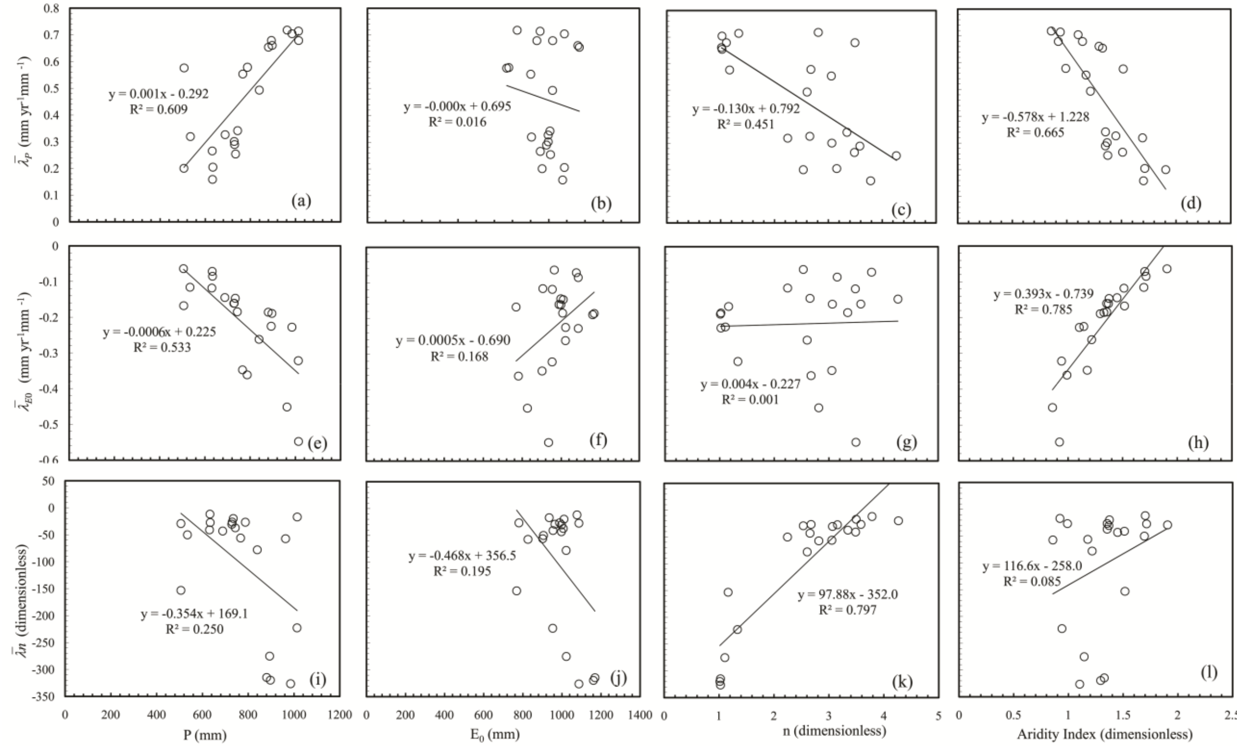

Fig. 7. $\overline{\lambda_P}$, $\overline{\lambda_{E0}}$ and $\overline{\lambda_n}$ in correlation with P, E_0, n, and aridity index.

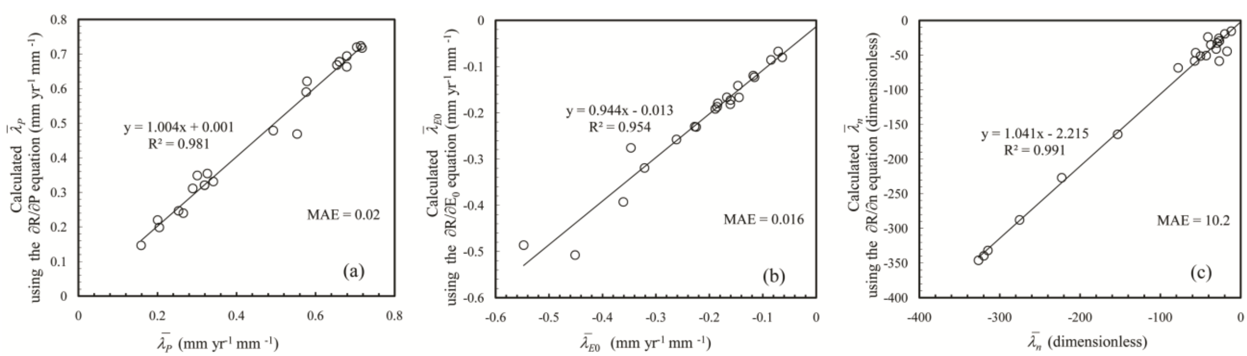

Fig. 8. Comparisons of $\overline{\lambda_P}$, $\overline{\lambda_{E0}}$ and $\overline{\lambda_n}$ (given in Table 4) with those predicted using Eq. (2) with the long-term mean values of P, E_0, and n as inputs. $MAE = N^{-1}\sum_{i=1}^{N}\left|O_i - P_i\right|$, is the mean absolute error, where O and P are values that actually encountered (given in Table 4) and predicted using Eq. (2) respectively, and N is the number of selected catchments.

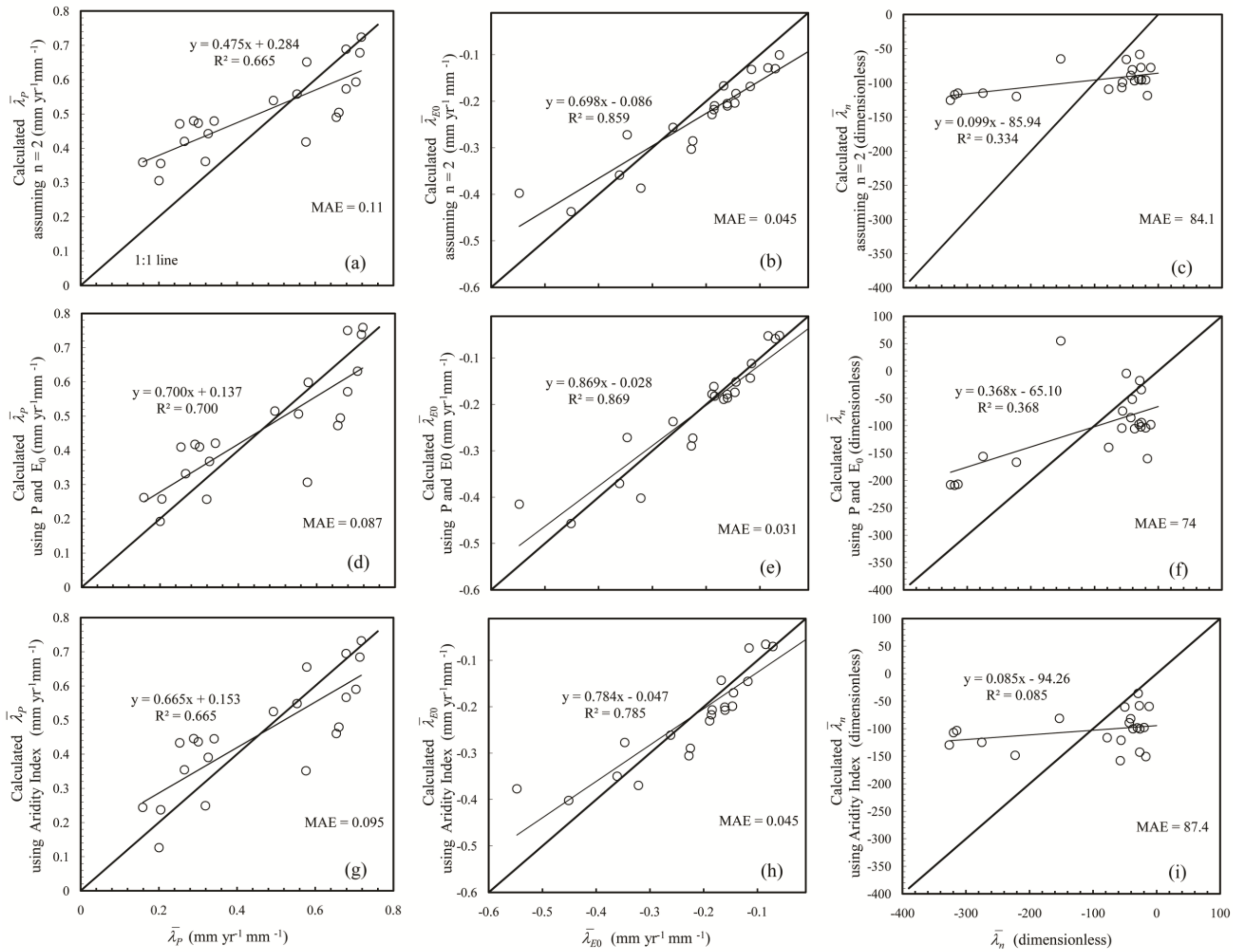

Fig. 9. Comparisons of $\overline{\lambda_P}$, $\overline{\lambda_{E0}}$ and $\overline{\lambda_n}$ with those predicted by the three strategies. (a)-(c) by Eq. (2) with a constant n (n = 2), (d)-(f) by the regression equations established using P and E_0: $\overline{\lambda_P} = 0.0011P - 0.0006E_0 + 0.21$ (R^2=0.7), $\overline{\lambda_{E0}} = 0.0007P - 0.0007E_0 - 0.38$ (R^2=0.87), and $\overline{\lambda_n} = -0.302P - 0.372E_0 + 493$ (R^2=0.37), and (g)-(i) by the regression equations established using only the aridity index, as shown in Fig. 7 (d), (h) and (l). *MAE* was calculated as for Fig. 8.